Iranian Journal of Science & Technology, Transaction B, Engineering, Vol. 31, No. B3, pp 289-301
Printed in The Islamic Republic of Iran, 2007

VOLTAGE SECURITY ENHANCEMENT AND CONGESTION MANAGEMENT VIA STATCOM & IPFC USING ARTIFICIAL INTELLIGENCE*

A. KARAMI, M. RASHIDINEJAD** AND A. A. GHARAVEISI

Dept. of Electrical Eng., Shahid Bahonar University of Kerman, Kerman, I. R. of Iran
Email: mrashidi@mail.uk.ac.ir

Abstract– Voltage security and congestion management are crucial issues in power systems, especially under heavily loaded conditions. In the new scheme of electricity restructuring, voltage security problems become even more serious. Due to the increase in stability margins, FACTS devices are the best option to mitigate voltage instability by reactive power management. The main purpose of this paper is to identify the optimal location and capacity of the Static Synchronous Compensator (STATCOM) to enhance voltage security and identify the capacity of a properly placed IPFC to manage transmission network congestion simultaneously. Artificial intelligence is implemented as a heuristic technique to this complicated constrained optimization problem. The proposed method demonstrates the improvement of the voltage security margin, as well as solving congestion management problems. Significant results through a modified IEEE 14-bus case study show the effectiveness of the proposed algorithm.

Keywords– Voltage security, congestion management, STATCOM, IPFC, RGA

1. INTRODUCTION

Voltage security is becoming an increasingly limiting factor in the planning and operation of many power systems. With increased system loading and open transmission access pressures, power systems are more vulnerable to voltage instability as shown by a number of major incidents throughout the world [1-3]. Flexible AC Transmission System (FACTS) controllers, on the other hand, are being used increasingly to provide voltage and power flow control in many utilities. The application to improve the voltage security margin in highly developed networks is well documented [4-6]. The implementation of FACTS technology, however, also merits attention in power systems with essentially longitudinal structures in developing countries. The last generation of FACTS controllers using the self commutated voltage source converter (VSC) usually includes the static synchronous compensator (STATCOM), static synchronous series compensator (SSSC), unified power flow controller (UPFC), and interline power flow controller (IPFC) [7-9]. STATCOM is mainly employed as a shunt reactive compensator and SSSC acts as a series active/ reactive compensator. UPFC provides a powerful tool for the cost-effective utilization of individual transmission lines by facilitating the independent control of both active and reactive power flow. However, UPFC and SSSC can control the power flow of only one transmission line. In comparison with UPFC and SSSC, IPFC has greater flexibility consisting of at least two converters where it can be used to control power flow in a group of lines. It can be anticipated that IPFC may be used to solve the complex transmission network congestion management problem, especially under transmission open-access environment. This is the case with the convertible static compensator (CSC) installed at the Marcy Substation of the New York Power Authority (NYPA) as a part of a project that will increase power transfer capability while maximizing the use of the existing transmission network [10, 11].

*Received by the editors January 31, 2007; final revised form April 25, 2007.
**Corresponding author

In this research, voltage security enhancement is modeled as an optimization problem. A STATCOM is allocated to a particular bus in order to improve the voltage security margin, while an IPFC is used to handle network congestion simultaneously. This paper is organized as follows: in section 2 the modeling of FACTS devices is described, and the optimization problem is defined and formulated in section 3. Real Genetic Algorithm (RGA) as an artificial intelligence is described in section 4. Section 5 presents the simulation results through a case study which is followed by concluding remarks in section 6**.**

2. FACTS DEVICES MODELING

FACTS devices offer a versatile alternative to conventional reinforcement methods with the potential advantages of increased flexibility, and lower operation and maintenance costs with less environmental influence. They will provide new control facilities, both in the steady state power flow control as well as dynamic stability control. The possibility of controlling power flow in electric power systems without generation rescheduling or topological changes can considerably improve the system performance. STATCOM and IPFC are those devices in which the modern power electronic converters have been employed. These converters are capable of generating reactive power with no need for large reactive energy storage elements. This can be achieved by making currents circulate through the phase of an AC system with the assistance of fast switching devices. The mathematical modeling of these two devices is developed mainly to perform the steady-state analysis in the next section.

a) Steady-state modeling of IPFC

It can be said that, IPFC with two or more converters may offer excellent voltage and a power flow control different from the concept of power flow control by a UPFC with two converters. As is shown in Fig. 1, IPFC is designed as a power flow controller with two or more independently controllable SSSC, which are solid-state voltage source converters (VSCs) injecting an almost sinusoidal voltage at variable magnitude, and are linked via a common DC capacitor. Conventionally, series capacitive compensation based on a fixed, thyristor controlled capacitor or SSSC is employed to increase the transferable active power on a given line in order to balance the loading of a transmission network [12]. In addition, active power can be exchanged through these two series converters via a common DC link in IPFC. It is noted that the sum of the active powers outputs from VSCs to transmission lines should be zero when the losses of the converter circuits can be ignored. A combination of the series connected VSC can inject a voltage with a controllable magnitude and phase angle at the fundamental frequency, while a DC link voltage can be maintained at a desired level. The common dc link is represented by a bidirectional link for active power exchange between voltage sources [13].

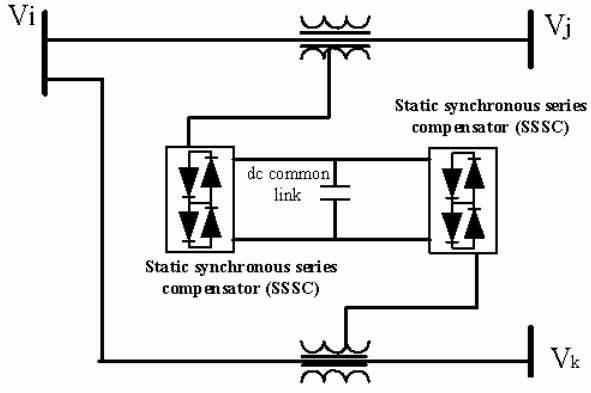

Fig. 1. Simplified schematic model of the IPFC

As illustrated in Fig. 2, a phasor diagram of voltage, for instance, controlled by one converter of IPFC defines the relationship between sending-end voltage ($\dot{V}_s$), receiving-end voltage ($\dot{V}_r$),voltage across line impedance X, ($\dot{V}_x$) and inserted voltage $\dot{V}_{pq}$ with a controllable magnitude as well as phase angle. When $\dot{V}_{pq}$ is added to the sending-end voltage, an effective sending-end voltage would be received as $\dot{V}_{seff} = \dot{V}_s + \dot{V}_{pq}$. Then the voltage difference ($\dot{V}_{seff} - \dot{V}_r$) sets the compensated voltage or $\dot{V}_x$ across reactance X. As ρ is varied over its full 360 degree range, the end of voltage $\dot{V}_{pq}$ moves along a circle with its center located at the end of voltage $\dot{V}_s$. The area within this circle defines the operating range of voltage $\dot{V}_{pq}$. According to the equivalent circuit of IPFC shown in Fig. 3, power flow equations can be obtained as follows:

$$P_i = V_i^2 g_{ii} - \sum_{j=1, j\neq i}^{n} V_i V_j (g_{ij}\cos(\theta_j - \theta_i) + b_{ij}\sin(\theta_j - \theta_i)) - \sum_{j=1, j\neq i}^{n} V_i Vse_{ij} (g_{ij}\cos(\theta_i - \theta se_{ij}) + b_{ij}\sin(\theta_i - \theta se_{ij})) \quad (1)$$

$$Q_i = -V_i^2 b_{ii} - \sum_{j=1, j\neq i}^{n} V_i V_j (g_{ij}\sin(\theta_j - \theta_i) - b_{ij}\cos(\theta_j - \theta_i)) - \sum_{j=1, j\neq i}^{n} V_i Vse_{ij} (g_{ij}\sin(\theta_i - \theta se_{ij}) - b_{ij}\cos(\theta_i - \theta se_{ij})) \quad (2)$$

$$P_{ji} = V_j^2 g_{jj} - V_i V_j (g_{ij}\cos(\theta_j - \theta_i) + b_{ij}\sin(\theta_j - \theta_i)) + V_j Vse_{ij} (g_{ij}\cos(\theta_j - \theta se_{ij}) + b_{ij}\sin(\theta_i - \theta se_{ij})) \quad (3)$$

$$Q_{ji} = -V_j^2 b_{jj} - V_i V_j (g_{ij}\cos(\theta_j - \theta_i) - b_{ij}\cos(\theta_j - \theta_i)) + V_j Vse_{ij} (g_{ij}\cos(\theta_j - \theta se_{ij}) \quad (4)$$

According to the operating principle of an IPFC [14], the active power exchange between series connected inverters via the common DC link is:

$$P_{sum} = \sum_{j=1, j\neq i}^{n} \{\mathrm{Re}(Vse_{ij}\bar{I}_{ij}\} = 0 \quad (5)$$

or

$$P_{sum} = \sum_{j=1, j\neq i}^{n} (Vse_{ij}^2 g_{ij} - V_i Vse_{ij} (g_{in}\cos(\theta_i - \theta se_{ij}) - b_{in}\sin(\theta_i - \theta se_{ij}))) + \sum_{j=1, j\neq i}^{n} (V_j Vse_{ij} (g_{in}\cos(\theta_j - \theta se_{ij}) - b_{ij}\sin(\theta_i - \theta se_{ij}) \quad (6)$$

Under the boundary constraints of the injected voltage source the following equations can be written.

$$V_{se_{ij}}^{\min} \le V_{se_{ij}} \le V_{se_{ij}}^{\max} \quad (7)$$

$$V_{se_{ij}}^{\min} \le V_{se_{ij}} \le V_{se_{ij}}^{\max} \quad (8)$$

$$\theta_{se_{ij}}^{\min} \le \theta_{se_{ij}} \le \theta_{se_{ij}}^{\max} \quad (9)$$

Where

$$g_{in} + jb_{in} = 1/Zse_{in}, g_{nn} + jb_{nn} = 1/Zse_{nn} \quad (10)$$

$$g_{ii} = \sum_n g_{in}, b_{ii} = \sum_n b_{in} \quad (11)$$

and

P_{ij} :active power flow from node *j* to node *i*

θ_{se} : angle of injected voltage

V_{se} : magnitude of injected voltage of FACTS controllers

θ :bus angle

V :bus voltage magnitude

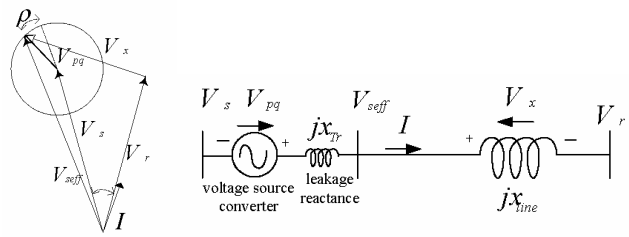

Fig. 2. Phasor diagram of voltage control

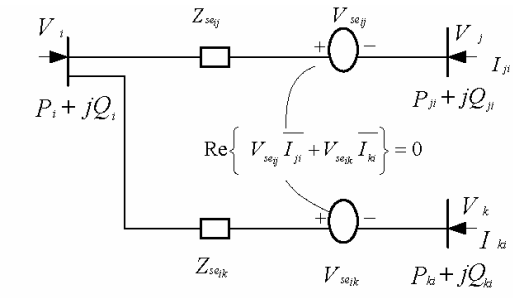

Fig. 3. Equivalent circuit of the IPFC

b) Steady-state modeling of STATCOM

STATCOM is based on the principle that a self-commutating inverter can be connected between three-phase AC power lines and is controlled to draw mainly reactive current from transmission lines. The current can be controlled to be either capacitive or inductive, which is rarely affected by the line voltage[15]. Therefore it provides much better performance of reactive compensation over the conventional SVC. A STATCOM circuit is shown in Fig.4, in which the DC part is described by the following differential equation [16].

$$\dot{V}_{dc} = \frac{P}{CV_{dc}} - \frac{V_{dc}}{R_C C} - \frac{R(P^2 + Q^2)}{CV^2 V_{dc}} \tag{12}$$

Power injection at the AC bus to which the STATCOM is connected has the following form:

$$P = V^2 G - kV_{dc} VG\cos(\theta - \alpha) - kV_{dc} VB\sin(\theta - \alpha) \tag{13}$$

$$Q = -V^2 B + kV_{dc} VB\cos(\theta - \alpha) - kV_{dc} VG\sin(\theta - \alpha) \tag{14}$$

Where: $k = \sqrt{\frac{3}{8}}m$.

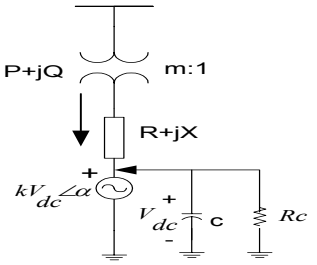

Fig. 4. STATCOM equivalent circuit

3. PROBLEM DEFINITION AND FORMULATION

Nonlinear dynamical systems such as those obtained from certain power system models can be generically described by the following ordinary differential equations:

$$\dot{X} = F(X, \lambda, \rho) \tag{15}$$

Where,

$x \in R^n$ corresponds to state variables

$\lambda \in R^1$ represents a particular set of non-controllable parameters that drive the system to bifurcation in a quasi-static manner. λ causes the system to steadily move from one equilibrium point to another. $\rho \in R^K$ represents a series of controllable parameters associated with control settings. Here λ is the distance

between the operating and the voltage collapse points. The maximum λ will be determined through an optimization process employing FACTS devices. The optimization problem can be formulated as:

$$\begin{aligned} &\text{M}in \quad F(u)=-\frac{1}{2}\|\lambda-\lambda_0\|_2 \\ &\text{S.t} \quad C(u)=\begin{bmatrix} F(x,\lambda,\rho) \\ D_x^T F(x,\lambda,\rho)w \end{bmatrix}=0 \\ &\qquad g_i(z)\le 0 \\ &\qquad u=(x,\lambda,w,\rho) \end{aligned} \tag{16}$$

where, $D_xF|_*$, is system Jacobian

W is normalized right zero eigenvectors in R^n of $D_xF|_*$.

$g_i(z)$ are inequality constraints such as voltage limitation.

The idea of this formulation is to maximize the distance between a given operating point defined by λ_0 and the collapse point [16, 17]. Control variables in this problem are the location and the capacity of STATCOM, as well as the capacity of IPFC. These variables are defined in relation to the optimization problem that can be represented by Eq. (17):

$$\begin{aligned} &\text{M}in \quad F(u) = -\frac{1}{2}\|\lambda-\lambda_0\|_2 \\ &St.\begin{cases} P_{Gi}-P_{Di}-\sum_{j=1}^{n}|V_i||V_j|(G_{ij-FACTS}\cos\delta_{ij}+B_{ij-FACTS}\sin\delta_{ij})=0 \\ Q_{Gi}-Q_{Di}-\sum_{j=1}^{n}|V_i||V_j|(G_{ij-FACTS}\sin\delta_{ij}-B_{ij-FACTS}\cos\delta_{ij})=0 \\ |V_i|_{\min}\le|V_i|\le|V_i|_{\max} \\ S_{ij}\le S_{ij}^{\max} \\ P_{G_{\min}}\le P_{G_i}\le P_{G_{\max}} \qquad i=1,\dots,N_G \\ Q_{G_{\min}}\le Q_{G_i}\le Q_{G_{\max}} \qquad i=1,\dots,N_G \\ 0\le V_{kpq}\le V_{kpq\,\max} \qquad i=1,\dots,M \end{cases} \end{aligned} \tag{17}$$

P_{Gi} and Q_{Gi} are real and reactive power generation at bus i. P_{Di} and Q_{Di} are real and reactive load demand at bus i, where n is total number of buses, $|V_i|$ is voltage magnitude at bus i, $G_{ij\text{-}FACTS}$ and $B_{ij\text{-}FACTS}$ are real and imaginary parts of the ij^{th} element of the Y_{bus} matrix including FACTS devices. S_{ij} is the apparent power flow in line ij, where $S_{ij\,max}$ is the thermal limit of line ij. N_G is the number of generators, P_{Gmax}& P_{Gmin}, and Q_{Gmax}& Q_{Gmin} are maximum and minimum real/ reactive power generation at bus i respectively. M is the number of converters in IPFC.

4. RGA AS AN OPTIMIZATION ALGORITHM

Genetic algorithm (GA) is one of the evolutionary algorithms in which individuals are called chromosomes. The value of an individual is fitness, which corresponds to the objective function that must be optimized. Unlike GA, real genetic algorithm (RGA) does not need any coding or decoding, and it seems to be faster and more accurate than binary GA [18, 19]. RGA operators including selection, recombination and mutation are explained in detail in the following sections.

a) Selection

In general, selection is based upon a random choosing process, where one well-known selection operator is called a roulette-wheel. Individuals are mapped to the adjacent segments of a line as shown in

Fig. 5. The length of each segment on this line corresponds to the fitness value of each individual. A random number will be generated and the individual whose segment spans the random number will be selected (trial). This technique is analogous to a roulette-wheel in which each slice is proportional in size to the fitness value.

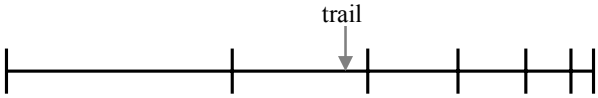

Fig. 5. Roulette-wheel operator

Ranking roulette-wheel selection: In the ranking selection the population is sorted according to the fitness values. The fitness assigned to each individual depends only on its position in the individuals' ranking, not on the actual fitness value. It is assumed that the number of individuals in a population is N, while p is the position of each individual in the population. To calculate the rank of each individual Eq. (18) can be used. In Eq. (18), the minimum and maximum value of P is 1 and N respectively, while SP a random number between 1 and 2 is illustrated in Fig. 6.

$$\text{Rank(P)} = 2 - \text{SP} + \frac{2(\text{SP} - 1)(\text{P} - 1)}{\text{N} - 1} \tag{18}$$

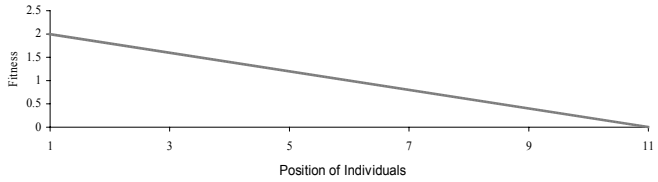

Fig. 6. Fitness assignment via ranking

b) Recombination

Recombination occurs when one of the RGA operators creates the next generation. This makes RGA different from binary GA. In this paper three kinds of recombination techniques, according their characteristics and performances, are used [18, 19]. Equations (19), (20), and (21) show these three recombination models.

$$\begin{aligned} O_1 &= \lambda P_1 + (1-\lambda) P_2 \\ O_2 &= \lambda P_2 + (1-\lambda) P_1 \qquad \lambda \in [0,1] \end{aligned} \tag{19}$$

$$\begin{aligned} O_1 &= \lambda_1 P_1 + (1-\lambda_1) P_2 \\ O_2 &= \lambda_2 P_2 + (1-\lambda_2) P_1 \qquad \lambda_1, \lambda_2 \in [0,1] \end{aligned} \tag{20}$$

$$\begin{aligned} O_1 &= \lambda \ P_1 + (1-\lambda) P_2 \\ O_2 &= \lambda P_2 + (1-\lambda) P_1 \qquad \lambda \in [-0.25, 1.25] \end{aligned} \tag{21}$$

Where, P_1, P_2 are the two parents, O_1, O_2 are their two offspring and λ_1, λ_2 are two random numbers. A typical individual chromosome with two genes is shown in Fig. 7. It is assumed that two parents with the same structure of Fig. 7 can be combined based upon different schemes. These schemes, which are related to Eqs. (19)-(21), are illustrated in Fig. 8. Figure 8a illustrates two parents under this condition, while Figures 8b-1, 8b-2 and 8b-3 represent Eqs. (19)-(21), schematically. Recombination based on Fig. 8b-1 generates offspring located on the corners of the hypercube defined by the parents. Line recombination, which is shown in Fig. 8-b2 can generate any point on the line defined by the parents. Fig.8b-3 shows the

intermediate recombination that is capable of producing any point within a hypercube slightly larger than that defined by the parents.

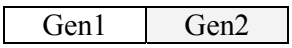

Fig. 7. Typical chromosome

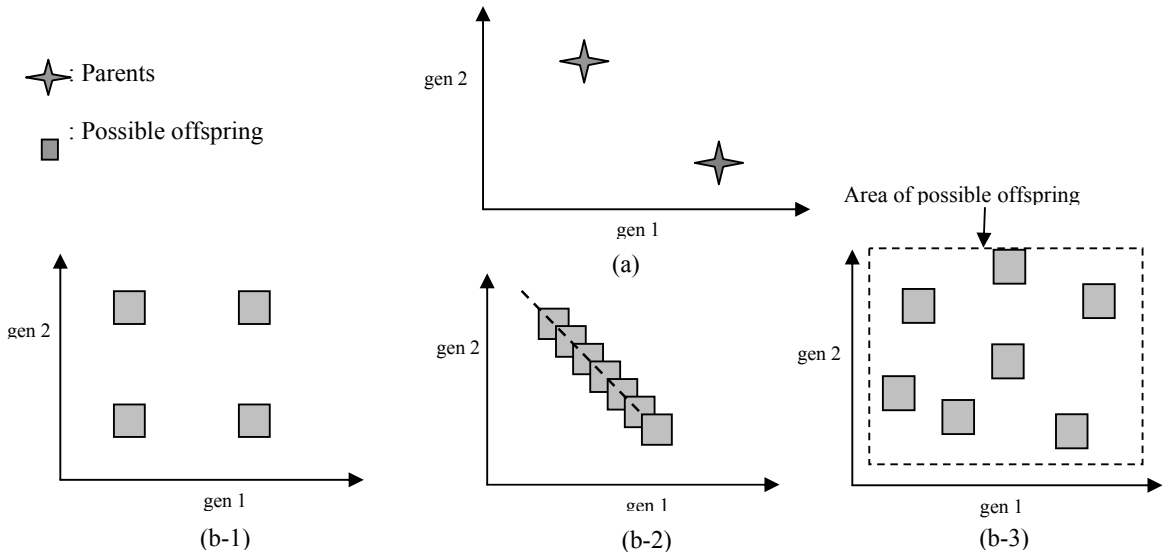

Fig. 8. Different schemes of recombination

c) Mutation

Mutation is for introducing artificial diversification into the population to avoid premature convergence which corresponds to a local optimum. An arithmetic mutation operator is a dynamic or non-uniform mutation that has been successfully used in a number of studies, where in this paper it is designed for fine-tuning aimed at achieving a high degree of precision. For a given parent P, if gene P_k is selected for mutation, then the resulting gene is selected with equal chance from the following two choices [20]:

$$\begin{cases} O_k = P_k - r(P_k - a_k)(1 - \frac{t}{T})^c \\ O_k = P_k + r(b_k - P_k)(1 - \frac{t}{T})^c \end{cases} \quad (22)$$

Where, a_k and b_k are the lower and upper band of P_k, r is a uniform random number between 0 and 1, t is the number of the current generation, T is the maximum number of the generation, and c is a parameter determining the degree of non-uniformity

d) Proposed algorithm

Figure 9 illustrates the flow chart of the optimization diagram in this study. The proposed algorithm includes two stages where, in the first stage the types, and the number of FACTS devices will be selected from a set of STATCOM and IPFC devices, while in the second stage, RGA will be run. Here the crossover and mutation rate are assumed 75 percent and 3 percent respectively. The second stage will be repeated until the algorithm is converged, while the results are the best location and the optimum rating for STATCOM as well as the optimum capacity of IPFC.

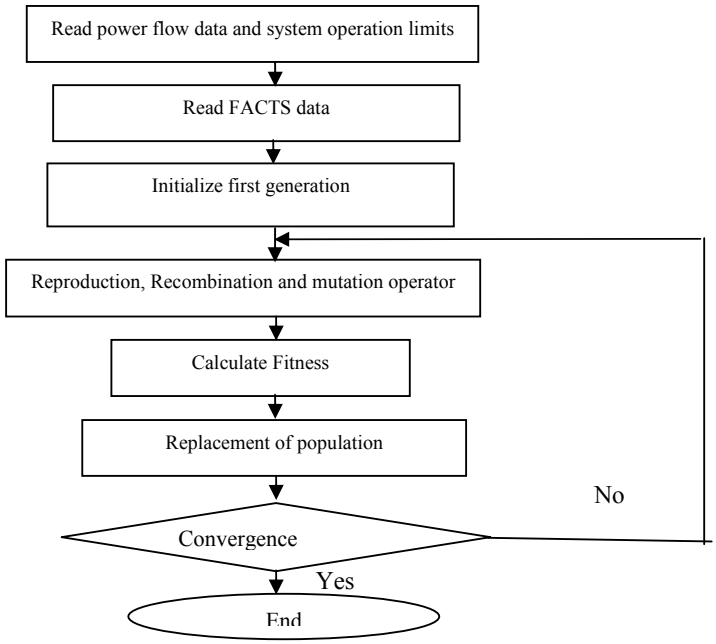

Fig. 9. RGA optimization flow diagram

5. CASE STUDIES & RESULTS ANALYSIS

In order to study the performance of a FACTS device one STATCOM is used to enhance the voltage security margin and one IPFC is employed to handle congestion management. Simulation was carried out on a modified IEEE 14-Bus system using a single diagram (the related data can be found in the appendix). The impact of using a STATCOM and an IPFC together is studied on the modified IEEE 14-Bus considering normal condition as well as applying a single contingency.

a) Base case with normal condition

The definition of base-case here is done without installing any FACTS devices, while STATCOM and IPFC are modeled as presented in section 2. The schematic connection diagram of IPFC is shown in the appendix. There is an overloaded branch (ln_2_4) connected to bus 4 with a loading percentage much higher than the other branches (ln_3_4 & ln_2_4) connected to the same bus. An IPFC is connected to the lines: ln_2_4, ln_3_4 & ln_4_5 via its 3 converters. Table 1 shows the loading percentage in the normal condition with the presence of IPFC. By connecting an IPFC between these branches, the overloading problem at branch (ln_2_4) is alleviated. The optimal values for converter 1, converter 2 and converter 3 derived from the optimization algorithm are: 123 MVA, 93 MVA and 48MVA, respectively. The total required capacity of IPFC is the sum of the MVAs of these three converters, which is 264 MVA.

Table 1. Loading percentage for normal case

Line-Name	Without IPFC %	With IPFC %
Ln_2_4	102.77	79.13
Ln_3_4	17.2	21
Ln_5_4	22.58	34.82

To improve the voltage security margin, the best location of STATCOM derived from the second stage of the optimization process is at bus 14 with the optimum capacity of 40 MVAr. The voltage profile is improved significantly (Fig. 10). The schematic diagram for the connection of STATCOM is shown in the

appendix. It can be seen that voltage collapse occurs at bus 14 in both the normal condition and after installing STATCOM. PV curves for the weakest bus (bus 14) in the base-cases & in the optimal case are depicted in Fig.11. From Fig. 11, it can be seen that the distance to the critical point of the PV curve, referred to as the voltage collapse point in the presence of STATCOM, increased by 55 MW.

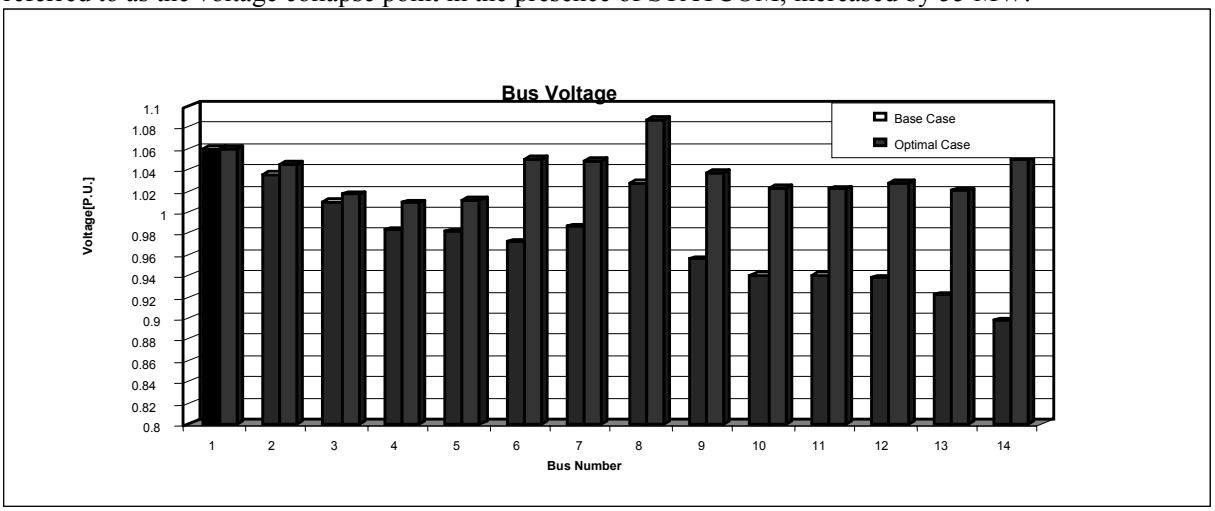

Fig. 10. Voltage profile with/ without STATCOM

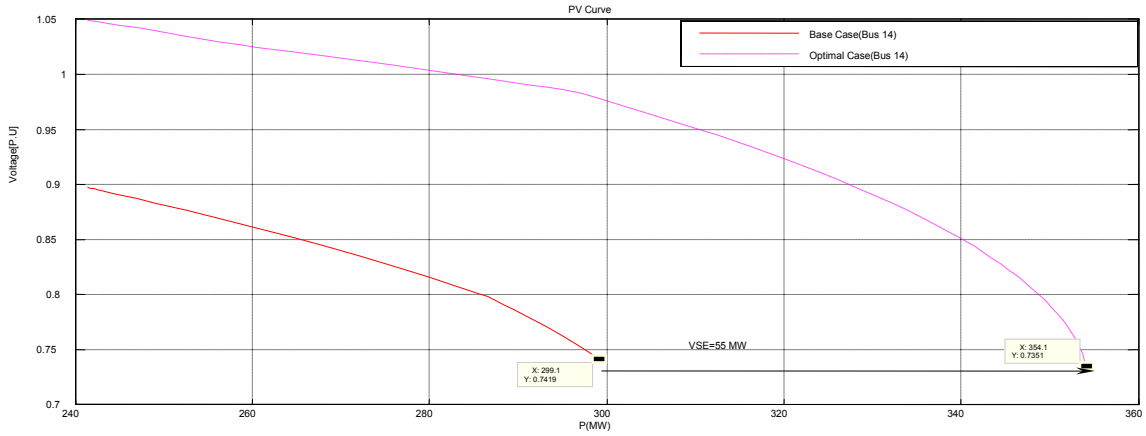

Fig. 11. PV curve at bus 14 with/ without STATCOM

b) Single contingency

In this section, the impact of single contingency on voltage security and congestion management in the presence of STATCOM& IPFC is studied under two scenarios.

1. Scenario 1: The worst single contingency resulting from contingency analysis occurrs when the line between buses 9&14 is disconnected. The voltage profile is shown in Fig.12 where it is improved significantly by employing these FACTS devices. It can be seen that the voltage collapse occurs at bus 14 both in the normal condition and after installing STATCOM. PV curves for the weakest bus (bus 14) in base-case & the optimal cases are depicted in Fig.13. As it is shown, the distance to the critical point of the PV curve under this condition with the presence of STATCOM increased by 72 MW.

2. Scenario 2: To investigate of the impact of using IPFC, a line between buses 4&5 (ln_4_5) is disconnected. In the base-case, the current loading of this line is 22.58%, which is between the loading of

the two other lines (ln_3_4 & ln_2_4). After contingency, the loading of ln_2_4 will increase to 114.91 %, while by installing IPFC between these three lines, it will be reduced to 95.31%. Table 2 shows the loading percentage in the base-case as well as in the presence of IPFC considering line contingency.

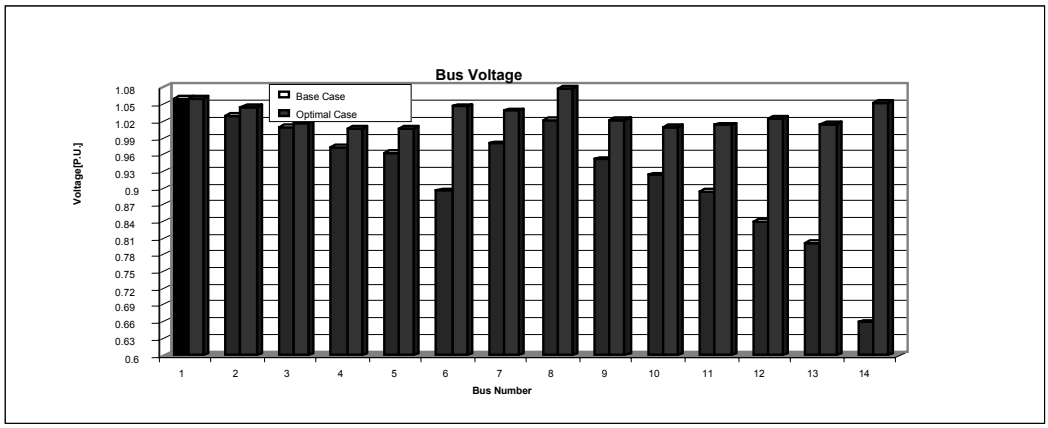

Fig. 12. Voltage profile with/ without STATCOM

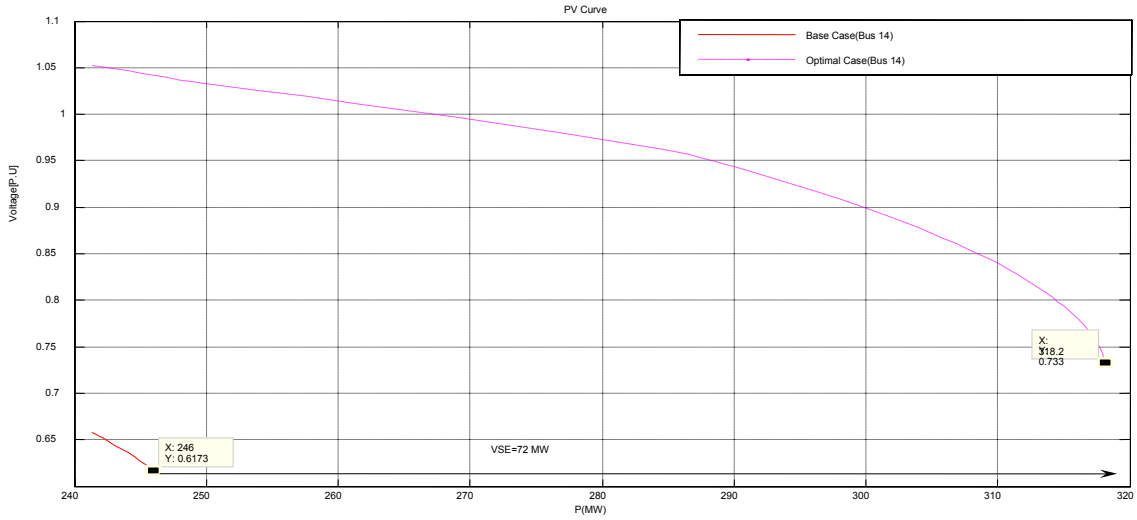

Fig. 13. PV curve at bus 14 with/ without STATCOM

Table 2. Loading percentage with line contingency

Line-Name	Without IPFC (%)	With IPFC (%)
Ln_2_4	114.91	95.31
Ln_3_4	18.87	29
Ln_5_4	0	0

6. CONCLUDING REMARKS

In this paper, the voltage security margin is enhanced by using STATCOM, while transmission congestion is managed via IPFC. RGA as a heuristic optimization algorithm is proposed to determine the optimal location of STATCOM and the optimum capacity for STATCOM and IPFC. The proposed methodology can handle voltage security and congestion management problems via a new generation of FACTS devices. These devices have effective roles in both normal and abnormal conditions such as contingency. It should be emphasized that under line contingency, even for the worst case, STATCOM and IPFC can

improve the voltage security margin as well as congestion relief. Simulation results through a modified IEEE 14-bus validates the effectiveness of the optimal placement as well as the best rating for these devices significantly.

REFERENCES

1. Natessan, R. & Radman, G. (2004). Effects of STATCOM, SSSC and UPFC on voltage stability. *IEEE Transaction on Power Systems, 4*(1), 546-550.
2. Canizares, C. A., Alvarado, F. L., DeMarco, C. L., Dobson, I. & Long, W. F. (1992). Point of collapse methods applied to ac/dc power systems. *IEEE Transaction on. Power Systems, 7*(2), 673-683.
3. Perez, M. A. & Fuert, C. A. (2000). Application of FACT devices to improve steady state voltage stability. *IEEE Trans Power Systems, 3*(2), 1115-1120.
4. Bulk Power System Voltage Phenomena-Voltage Stability and Security, (1989). EPRI Research Project 2473-21.
5. Kundur, P., Morison, K. & Gao, B. (1993). Practical consideration in voltage stability assessment. *Electrical Power &Energy Systems, 15*(4), 205-215.
6. Sen, K. K. (1998). SSSC-static synchronous series compensator theory, modeling and application. *IEEE Trans. Power Del., 13*(1), 241–246.
7. Sen, K. K. (1998). UPFC-unified power flow controller theory-modeling and applications. *IEEE Trans. Power Del., 13*(4), 453–1460.
8. Schauder, C. D., Lund, M. R., Hamai, D. M., Rietman, T. R., Torgerson, D. R. & Edris, A. (1998). Operation of the unified power flow controller (UPFC) under practical constraints. *IEEE Trans. Power Del., 13*(2), 630–637.
9. Gyugyi, L., Sen, K. K. & Schauder, C. D. (1999). The interline power flow controller concept a new approach to power flow management intransmission systems. *IEEE Trans. Power Del.*, *14*(3), 1115–1123.
10. Zelingher, S., Fardanesh, B., Shperling, B., Dave, S., Kovalsky, L., Schauder, C. & Edris, A. (2000). Convertible static compensator project—hardware overview. *Proc. IEEE Winter Meeting*, 2511–2517.
11. Arabi, S., Hamadanizadeh, H. & Fardanesh, B. (2002). Convertible static compensator performance studies on the NY state transmission system. *IEEE Trans. Power Sysemt.*, *17*(3), 701–706.
12. Zhang, Y. & Chen, C. (2006). A novel power injection model of IPFC for power flow analysis inclusive of practical constraints. *IEEE Trans On Power Systems, 21*(4), 1550-1556.
13. Hingorani, N. G. & Gyugyi, L. (1999*). Understanding FACTS: concepts and technology of flexible AC transmission systems*. Wiley-IEEE Press.
14. Wei, X., Chow, J. H., Fardanesh, B. & Edris, A. A. (2002). A dispatch strategy for an interline power flow controller operating at rated capacity. *14th PSCC*, Sevilla, Spain.
15. Das, J. C. (2002). *Power system analysis short–circuit load flow and harmonics*. Marcel Dekker, Inc.
16. Canizares, C. A. (2000). Power flow and transient stability models of FACTS controller for voltage and angle stability studies. *IEEE Trans on Power System, 5*(6), 1447-1454.
17. Canizares, C. A. (1998). Application of optimization to voltage collapse analysis. *IEEE/PES Summer Meeting*, 1-8.
18. Feng, W. & Shrestha, G. B. (2001). Allocation of TCSC devices to optimize total transmission capacity in a competitive power market. *Power Engineering Society Winter Meeting, 2001. IEEE, 2*, 587 – 593.
19. Janikow, C. Z. & Michalewicz, Z. (1993). An experimental comparison of binary and floating point representation in genetic algorithm. *Proc. of International Forth Conference on Genetic Algorithm*, 31-36.
20. Pingkang, L., Xiuxia, D. & Yulin, L. (2002). AGC parameter optimization using real coded genetic algorithm. Power System Technology, *Proceedings. Power Con, 1*, 646-650.

APPENDIX

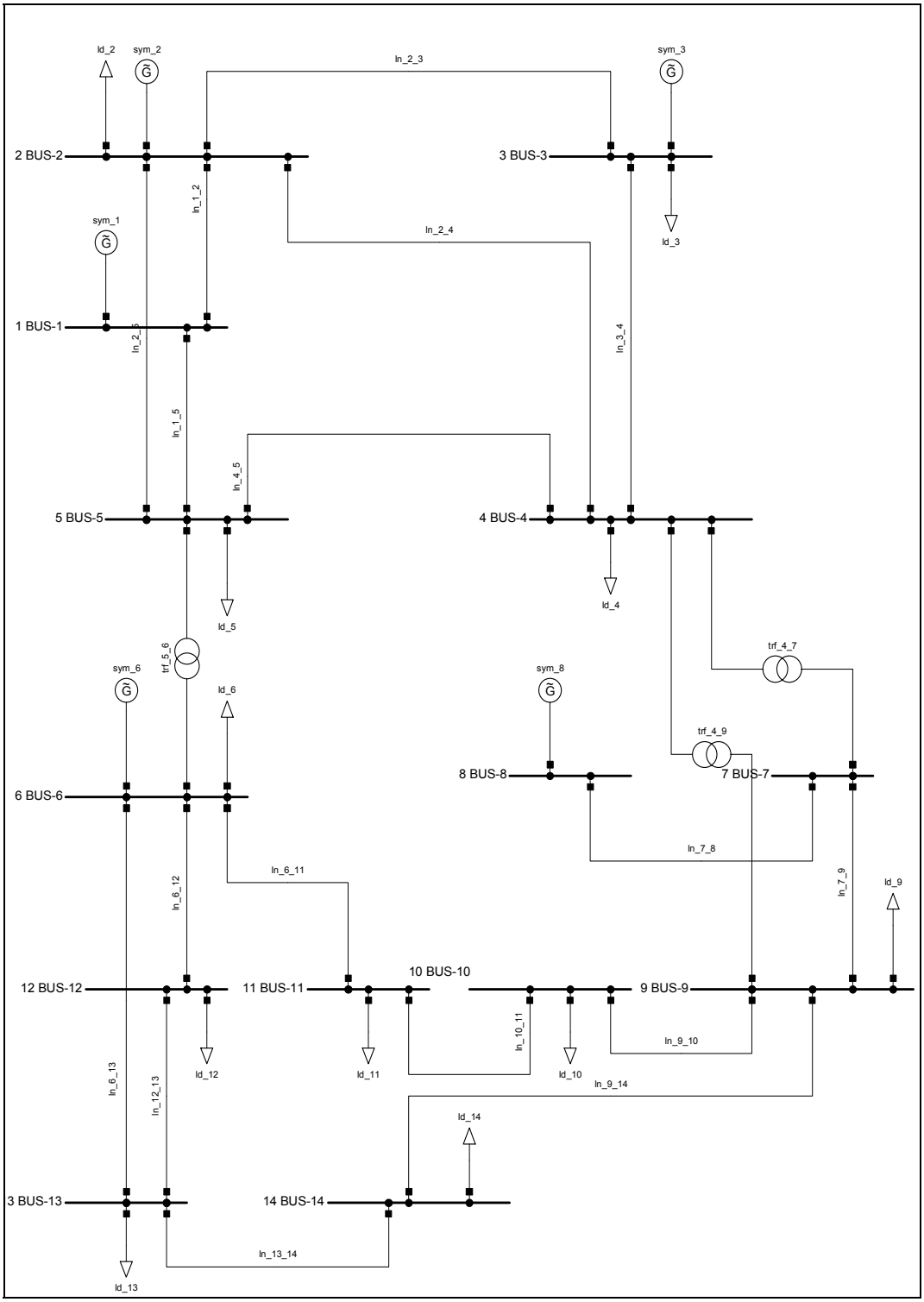

Fig. 14. Single line diagram of a modified IEEE 14-bus

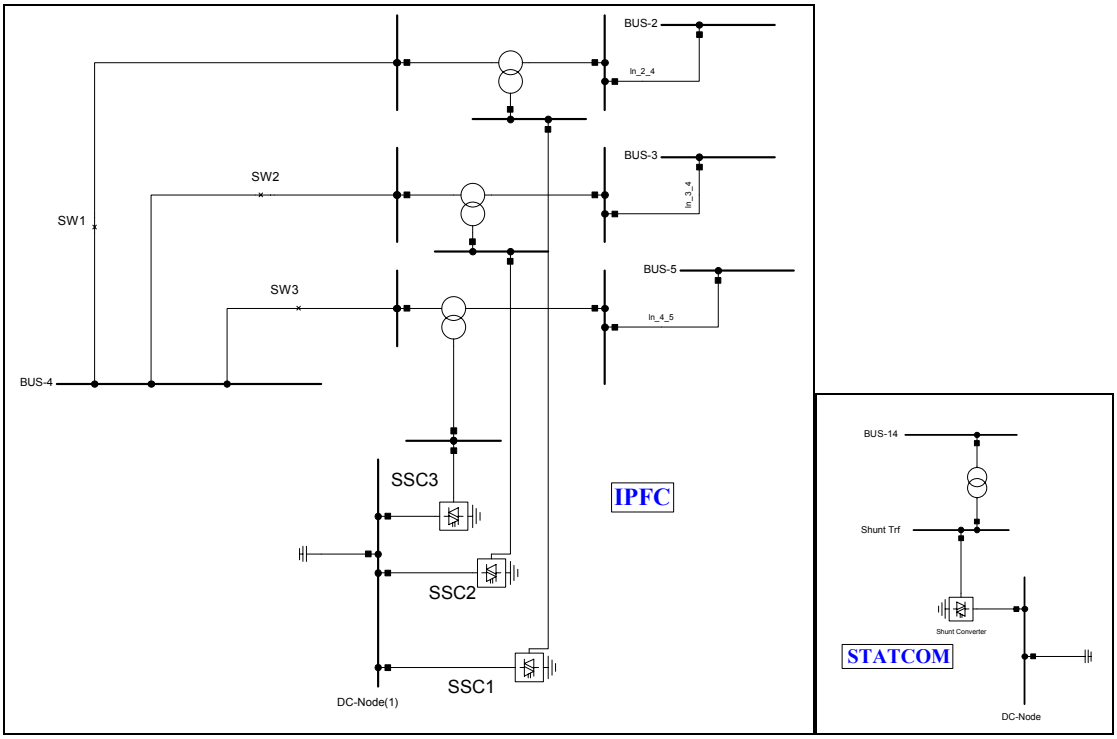

Fig. 15. Schematic diagram of IPFC & STATCOM connected to lines originated from bus 4 & 14

Table 1. Line data

Line	$R_1(\Omega)$	$X_1(\Omega)$
ln_1_2	1.938	5.917
ln_1_5	5.403	22.304
ln_2_3	4.699	19.797
ln_2_4	3.811	7.632
ln_2_5	5.695	17.388
ln_3_4	6.701	17.103
ln_4_5	1.335	4.211
ln_6_11	9.498	19.89
ln_6_12	12.291	25.581
ln_6_13	6.615	13.027
ln_7_8	0	17.615
ln_7_9	0	11.001
ln_9_10	3.181	8.45
ln_9_14	12.711	27.038
ln_10_11	8.205	19.207
ln_12_13	22.092	19.988
ln_13_14	17.093	34.802

Table 2. Load data

Load	Active Power MW	Reactive Power Mvar
ld_2	4.10728	2.38168
ld_3	16.14128	4.7096
ld_4	50.1894	-6.1347
ld_5	11.9548	2.5168
ld_6	17.6176	11.7975
ld_9	35.4035	13.1118
ld_10	20.157	9.1234
ld_11	15.5055	7.8314
ld_12	9.5953	2.5168
ld_13	31.2355	17.1234
ld_14	24.4377	13.865